

# Oxidative Polymerization of Pyrrole Photocatalyzed by TiO<sub>2</sub> Nanoparticles and Interactions in the Composites

Zhen Weng, Xiuyuan Ni

The Key Laboratory of Molecular Engineering of Polymer of State Educational Minister,  
Department of Macromolecular Science, Fudan University, Shanghai 200433, China

Received 20 July 2007; accepted 24 April 2008

DOI 10.1002/app.28636

Published online 13 June 2008 in Wiley InterScience (www.interscience.wiley.com).

**ABSTRACT:** Oxidative polymerization of pyrrole is initiated by photoexcited TiO<sub>2</sub> nanoparticles. Pyrrole oligomers and polypyrrole (PPy) are continuously produced with reaction time. The conversion of pyrrole monomer changes as a function of the concentration of TiO<sub>2</sub> nanoparticles. It is found that PPy in the composite has the conjugated structure and is partially oxidized with a formation of positively charged N<sup>+</sup>. Results from X-ray photoelectron spectroscopy and Raman analysis consistently indicate that a strong interaction is estab-

lished between the TiO<sub>2</sub> and PPy. According to the results of UV-vis spectroscopy, a mechanism of photocatalytic oxidation is proposed for this polymerization. The interaction between TiO<sub>2</sub> and PPy is found to arise from the photocatalytic reaction and discussed in terms of photoinduced Ti<sup>3+</sup>. © 2008 Wiley Periodicals, Inc. *J Appl Polym Sci* 110: 109–116, 2008

**Key words:** photopolymerization; conjugated polymers; polypyrrole; nanocomposites

## INTRODUCTION

Conjugated polymers have substantial  $\pi$ -electrons delocalizing along their back bones, which give rise to special optical properties and allow the polymers to exhibit good electric conductivity.<sup>1,2</sup> Heterojunction composites of conjugated polymers and semiconductor nanoparticles (NPs) have received much attention owing to the recent interest in photoelectric devices including solar cells, photodiodes, and light-emitting diodes.<sup>3–5</sup> Photoelectric properties of this kind of composite essentially arise from synergic effects of the two components when the composite is imposed by a light excitation or electrical stimulation. Polypyrrole (PPy) is one of the most important conjugated polymers and is known for its higher conductivity and better ambient stability in practical devices.<sup>2,6–8</sup> As reported in literatures, PPy is synthesized by oxidative polymerization, in which various organic oxidants are used as initiators.<sup>1,2</sup>

Because the conjugated polymers, including PPy, are not molten in nature and generally are insoluble

in solvents, it is difficult to obtain the composites of conjugated polymers and semiconductor NPs by conventional blending or mixing methods. Several groups have reported a sol method<sup>9</sup> and *in situ* polymerization<sup>10</sup> for preparing the composites. However, a problem remains that the interface of the composites is not stabilized, because the resulting polymer simply deposits on the semiconductor NPs. As well known, a stabilized interface of the heterojunction composite is highly desired, because it favors not only the rate of charge injection when imposed by a light excitation or electrical stimulation<sup>8,11</sup> but also the lifetime of the photoelectric devices from the composite materials. Recent studies have synthesized soluble conjugated polymers and copolymers in order that the composites with more stable interface can be obtained by means of solution adsorbing and self-assembling. But, complex reaction procedures are usually required.<sup>12</sup>

UV excitation of semiconductor NPs yields the conduction-band electron ( $e^-$ ) and valence-band hole ( $h^+$ ) in pairs that perform surface-mediated redox.<sup>13</sup> Recently, it has been proven that the photoexcited semiconductor NPs are capable of catalyzing free-radical polymerizations of alkenes, that is, the polymerization is photocatalyzed by the semiconductor NPs.<sup>14–18</sup> We have shown the free-radical polymerization of methyl methacrylate initiated by photoexcited TiO<sub>2</sub> NPs and the reaction kinetics of the polymerization.<sup>14–16</sup> To the best of our knowledge, however, there is no attempt at oxidative polymerization by using the photoexcited semiconductor

Correspondence to: X. Ni (xyni@fudan.edu.cn).

Contract grant sponsor: National Nature Science Foundation of China (NSFC); contract grant number: 20574011.

Contract grant sponsor: Science and Technology Commission of Shanghai Municipality; contract grant numbers: 05nm05013, 055207080.

NPs. In this study, we successfully initiate the oxidative polymerization of pyrrole by using TiO<sub>2</sub> NPs in aqueous suspensions. This polymerization expands strategies to fabricate the heterojunction composites of conjugated polymers and semiconductor NPs and has the advantage of simple procedure, because semiconductor NPs directly participates into the synthesis of the composite. In particular, a strong interaction is observed in the as-prepared composite. Mechanisms about the polymerization and interaction are discussed in terms of semiconductor photocatalysis.

## EXPERIMENTAL

Degussa P25 TiO<sub>2</sub> (80% anatase and 20% rutile) with an average size diameter of 21 nm was used. Pyrrole was distilled before use. All the other chemicals used were of analytical reagent grade. Deionized water was used in the experiments.

P25 TiO<sub>2</sub> NPs were dispersed into aqueous solutions of pyrrole, using the ultrasonic dispersion technique. The mixture of 120 mL was moved into a quartz reactor that was equipped with a magnetic stirrer and a water jacket that is connected to a circulator of saturated CuSO<sub>4</sub> solution. The reactor was properly sealed to prohibit the reaction mixture from air. UV irradiation toward the reactor was carried out using a mercury vapor lamp, characterized by two chief peaks at 254 and 365 nm in its emission spectrum. The mixture can avoid being irradiated by the rays exclusive of 365 nm, due to the cutting off of CuSO<sub>4</sub> solution.<sup>14–16</sup> It was determined by a radiometry (UV-A, BJNU Photoelectrical Co.) that the intensity at the reactor position was 13 mW/cm<sup>2</sup> for 365 nm and 0.085 mW/cm<sup>2</sup> for 254 nm. The pyrrole aqueous solutions containing P25 TiO<sub>2</sub> NPs were subjected to the ultraviolet irradiation for different time. Darkish precipitations were obtained after a centrifugation of the reacted mixture, washed by water, and then dried under vacuum for 24 h.

UV–vis spectra of the reacted solutions were recorded on a Lambda 35 PerkinElmer UV–vis spectrophotometer in the range of 190–1100 nm, and the TiO<sub>2</sub> aqueous solution was used as reference. Fourier transform Raman spectra of the composites were recorded using a LabRam-1B (Dilor) Raman spectrometer. To examine possible influences of pyrrole absorption on TiO<sub>2</sub> Raman spectra, the TiO<sub>2</sub> sample kept wet by pyrrole during the measurements. Thermogravimetric analysis (TGA) of the composite was carried out with a PerkinElmer Pyris 1 TGA instrument at a heating rate of 15°C/min in air. X-ray photoelectron spectroscopy (XPS) analysis was carried out using a PHI-5000C ESCA system (PerkinElmer) with Al K $\alpha$  radiation ( $h\nu = 1486.6$  eV). The X-ray anode was run at 250 W, and the high voltage was kept at 14.0 kV with a detection angle at

54°. The pass energy was fixed at 46.95 eV to ensure sufficient sensitivity. The base pressure of the analyzer chamber was about  $5 \times 10^{-8}$  Pa. The sample was directly pressed to a self-supported disk (10 × 10 mm) and mounted on a sample holder and then transferred into the analyzer chamber. The whole spectra (0–1200 eV) and the narrow spectra of all the elements with much high resolution were both recorded. The data analysis was carried out by using the PHI-MATLAB software provided by PHI Corp.

## RESULTS AND DISCUSSION

### Pyrrole polymerization initiated by photoexcited TiO<sub>2</sub> nanoparticles

The UV–vis absorption of pyrrole is at  $\lambda_{\max}$  of 206 nm [Fig. 1(A)]. Because the UV light used in this study locates at the wavelength of 365 nm, it is unlike for

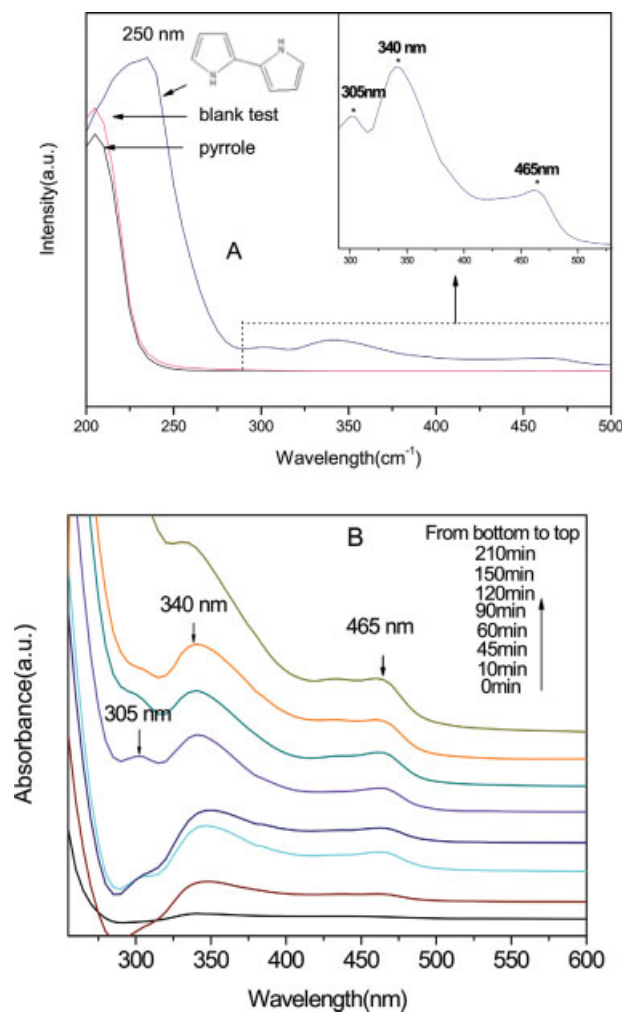
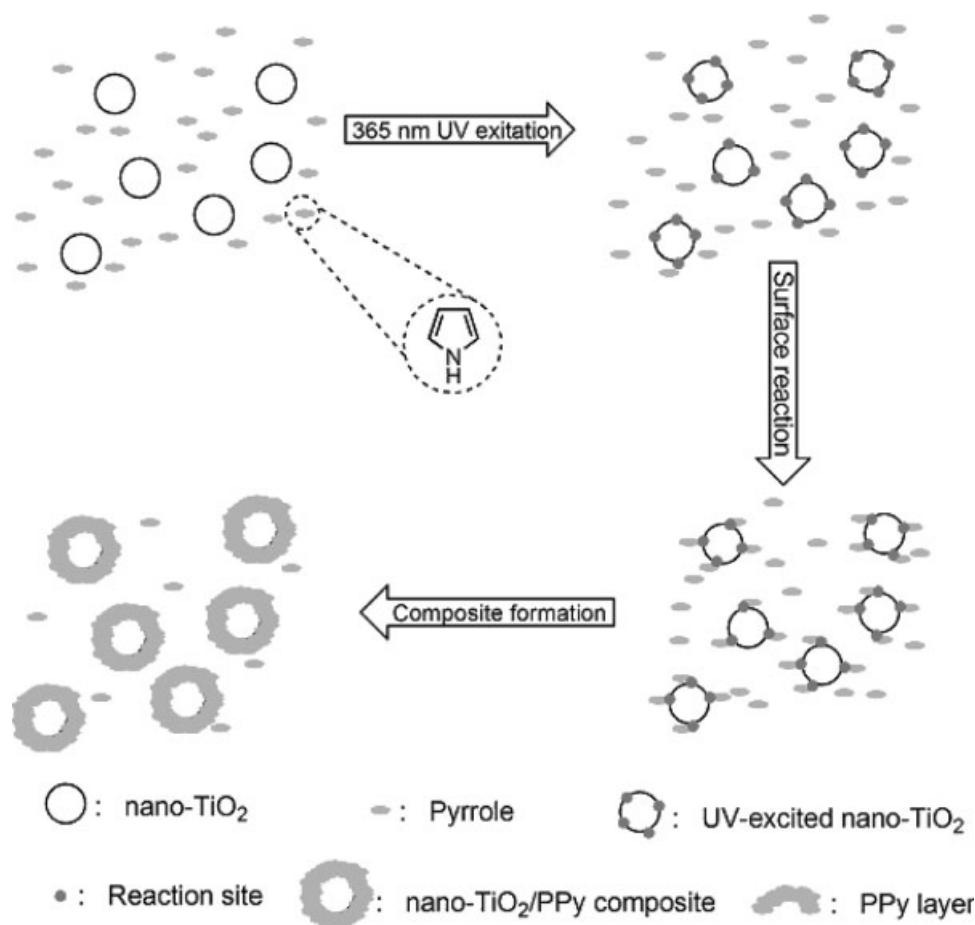


**Figure 1** UV–vis spectra of (A) pyrrole, blank test, and reaction solution with reaction time of 90 min; (B) reaction solution with different time. TiO<sub>2</sub> suspension with the same concentration and treatment process served as the background. [Color figure can be viewed in the online issue, which is available at [www.interscience.wiley.com](http://www.interscience.wiley.com).]



**Scheme 1** The schematic diagram of preparing polypyrrole-nanoscale TiO<sub>2</sub> composites through catalysis of photoexcited TiO<sub>2</sub> nanoparticles. [Color figure can be viewed in the online issue, which is available at [www.interscience.wiley.com](http://www.interscience.wiley.com).]

pyrrole to absorb this light. As shown in Figure 1(A), the intrinsic absorption of pyrrole keeps the same after the irradiation, indicating that the UV light used here brings about no chemical change to pyrrole as expected. It is important to see that when TiO<sub>2</sub> NPs is added, four absorption bands newly appear after the identical irradiation. The band centered at 250 nm is assigned to the pyrrole dimer. The bands at 305 and 340 nm are assigned to the terpyrrole and quarterpyrrole oligomers,<sup>19</sup> respectively. The broad band at 465 nm, which has been assigned to the  $\pi$ - $\pi^*$  transition of PPy,<sup>19-21</sup> indicates that PPy is produced. Considering that no polymerization occurs without TiO<sub>2</sub> NPs, the observed polymerization is due to the TiO<sub>2</sub> NPs that are photoexcited, because the UV light at 365 nm is sufficient to overcome TiO<sub>2</sub> band gap energy ( $E_g = 3.2$  eV<sup>13</sup>). Scheme 1 shows the synthesis route to the PPy/TiO<sub>2</sub> NPs composite.

Figure 1(B) shows that the absorption intensities of pyrrole oligomers and PPy increase with reaction time, indicating a continuous production of the oligomers and PPy. Figure 2 shows that the conversion of pyrrole is changed as a function of the con-

centration of TiO<sub>2</sub> NPs. It was observed in the experiments that the reaction solution turns dark more rapidly with the increase in the concentration of TiO<sub>2</sub>. This should prevent the incident light from

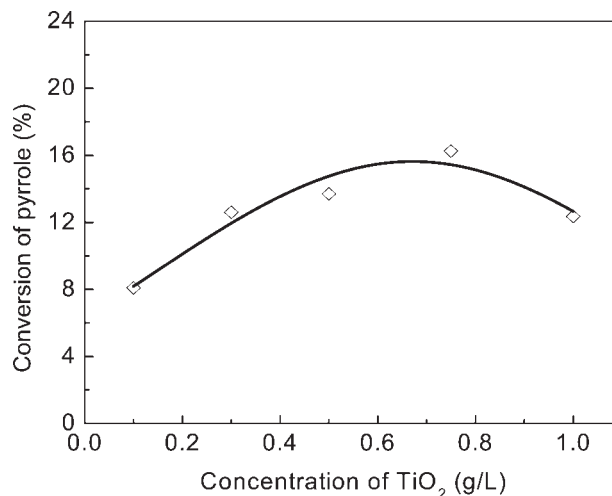


**Figure 2** The conversion of pyrrole versus the concentration of TiO<sub>2</sub>. The concentration of pyrrole was 0.01 mol/L.

reaching the TiO<sub>2</sub> during the subsequent reaction. It has been demonstrated that the efficiency of photocatalytic reaction increases with increasing the concentration of semiconductor NPs and depends on the quantum efficiency of the semiconductor, whereas the quantum efficiency is determined by the intensity of absorbed light.<sup>16</sup> We believe that the dependence of PPy yields on the TiO<sub>2</sub> concentration here results from the influences of the two factors. It is found that the polymerization is effectively initiated when the amount of TiO<sub>2</sub> is as low as 0.1 g/L. This result indicates high efficiency for the TiO<sub>2</sub> NPs in the aqueous suspension. Previous preparations of composites of PPy and semiconductor NPs can be summarized into two methods: one is to use organic oxidants to initiate pyrrole polymerization in the presence of semiconductor NPs; and the other is to synthesize soluble PPy polymers in order that the composites can be prepared by means of absorbing and self-assembling. In comparison, it seems that the method of this study has the advantage of simple fabrication process.

### Interaction in the composite

#### XPS analysis

High-resolution XPS analysis is used to characterize the resulted TiO<sub>2</sub>/PPy composite. Figure 3 shows the N 1s core levels obtained after the reaction for 45 and 90 min. Using the standard line-shape analysis, the N 1s spectrum is fitted with three components having the same full width at half-maximum (FWHM). The chemical environments of N atoms, corresponding to the three components, have been completely defined in literature as follows.<sup>22</sup> The major component at 399.8 eV is assigned to neutral pyrrolylium nitrogen (N—H). The low binding energy (BE) component at 397.9 eV is assigned to the imine nitrogen (=N—). The high-BE component at 402.9 eV is assigned to the positively charged nitrogen atom (—N<sup>+</sup>).<sup>22</sup> The presence of —N<sup>+</sup> indicates that the PPy component are doped, that is, PPy are in the oxidized state.<sup>22,23</sup> From the ratio, the peak area of N<sup>+</sup> to that of total N 1s orbital, it is calculated out that the doping level is about 20% at 45 min, that is, each five pyrrole rings in the chain has on average one linkage onto the TiO<sub>2</sub> NPs. This value is comparable to that hold by conventionally doped PPy.<sup>22,23</sup> The N<sup>+</sup> polaron is critical for PPy to exhibit conductive, because the direct electrostatic interaction of the positive charge and electron facilitates the conduction.<sup>24</sup> So, PPy in the composite would have good conductivity.

N<sup>+</sup> of PPy is usually achieved by incorporating Lewis acids as dopants into PPy.<sup>2,22</sup> According to the mechanism for the doping reaction,<sup>22</sup> the dopant,

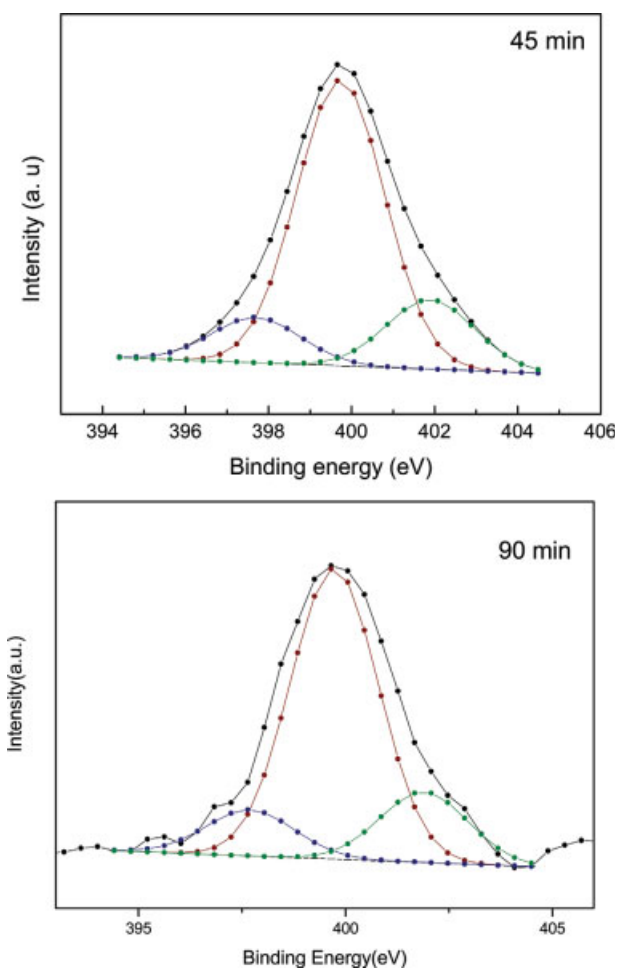


**Figure 3** XPS signal relevant to N 1s orbital recorded on composite synthesized with (A) 45 min and (B) 90 min. [Color figure can be viewed in the online issue, which is available at [www.interscience.wiley.com](http://www.interscience.wiley.com).]

serving as the electron acceptor, forms a complex with PPy, and a charge transfer occurs between the dopant and PPy (serving as the electron donor) leading to the structure of  $A^{\delta-} \dots D^{\delta+}$ , so that the complex keeps neutral. As a result, PPy is oxidized with the formation of —N<sup>+</sup>. Accordingly, the presence of N<sup>+</sup> in this study indicates that the TiO<sub>2</sub> is combined with PPy to form a complex. It should be mentioned that the UV-vis absorption at 465 nm (Fig. 1) is assigned to partially oxidized PPy with N<sup>+</sup>,<sup>19–21</sup> being consistent with the XPS result.

#### Raman analysis

Figure 4 shows the Raman spectra of the resulted composites and the reference PPy, which is synthesized using FeCl<sub>3</sub> as the initiator. The double bands centered at 1350 and 1600 cm<sup>-1</sup> typically belong to PPy.<sup>25</sup> The band centered at ~1350 cm<sup>-1</sup> is assigned to the stretching mode of pyrrole ring. Another band centered at 1560 cm<sup>-1</sup> is assigned to the C=C

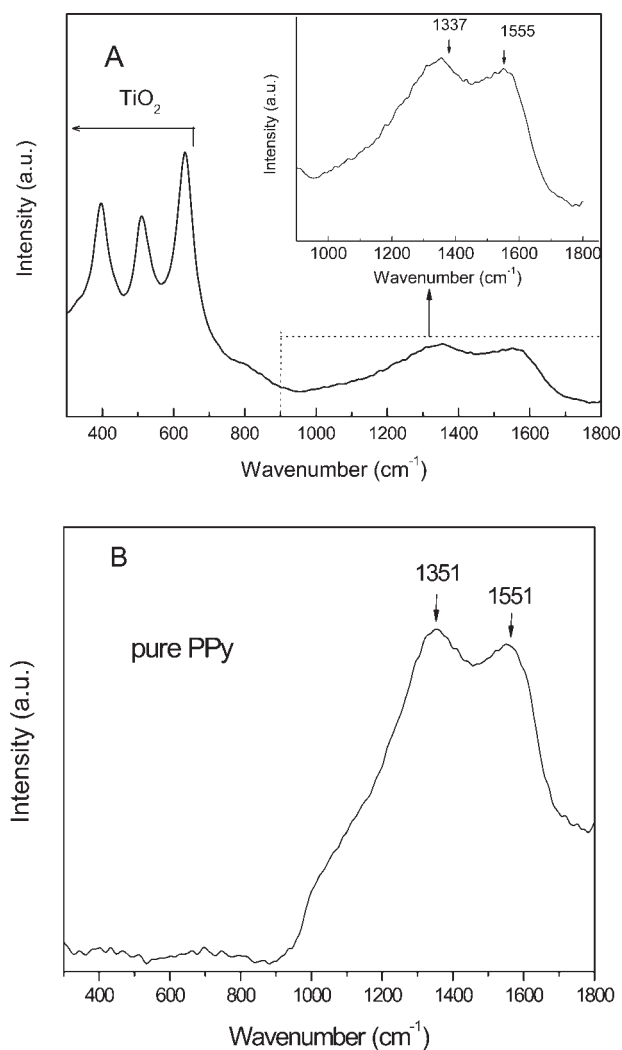


**Figure 4** Raman spectra of the composite this study (A) and reference polypyrrole synthesized using  $\text{FeCl}_3$  as initiator (B).

backbone stretching of PPY.<sup>25</sup> These observations not only confirm the synthesis of PPY in this study, but also show that the PPY has the typical conjugated structure.

Shown in Figure 5 is the Raman region of  $\text{TiO}_2$  obtained after the polymerizations for different time. The neat  $\text{TiO}_2$  is characterized by a strong and sharp band at  $146\text{ cm}^{-1}$ , three mid intensity band at  $399$ ,  $519$ , and  $640\text{ cm}^{-1}$ , and a weak band at  $200\text{ cm}^{-1}$ . The band at  $146\text{ cm}^{-1}$  is assigned to the bending type vibration of  $\nu_6$  ( $E_g$ ) mode.<sup>26</sup> It is found from Figure 5(A) that the band of  $146\text{ cm}^{-1}$  shows a blue shift by  $8\text{ cm}^{-1}$  for the composites when the reaction is beyond 10 min. Meanwhile, the FWHM of each band increases a lot, as shown in Figure 5(B) and tabulated in Table I. Importantly, the results reveal that the composite of  $\text{TiO}_2$  NPs and PPY is not a simple mixture, but the two components interact with each other. Taking the early XPS results into

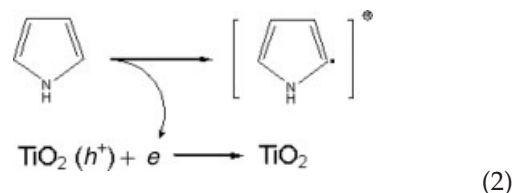
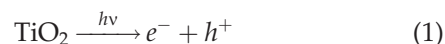
accounts, the two different spectroscopies consistently indicate that the interaction is established between the  $\text{TiO}_2$  and PPY.

It is realized here that Parker et al.<sup>27</sup> have addressed Raman shifts and broadening by comparing the  $\text{TiO}_2$  NPs having various O/Ti ratios. They found that when the O/Ti ratio decreased from 2 to 1.89, the blue shift of the  $\nu_6$  ( $E_g$ ) band increased to  $11\text{ cm}^{-1}$  continuously, whereas the FWHM increased from 12 to  $35\text{ cm}^{-1}$ . More recently, several authors have detected similar Raman shifts and broadening for modified  $\text{TiO}_2$  NPs including N-doped  $\text{TiO}_2$ <sup>28–30</sup> and concluded that the phenomena were due to the nonstoichiometric oxygen. The implication to us is that the surface structure of  $\text{TiO}_2$  in the composite varied due to the interaction.

### Mechanisms discussions

As mentioned in the Introduction, PPY is always synthesized by oxidative polymerization. The first step is that pyrrole is oxidized to pyrrole radical cation that is the key intermediate deciding the subsequent polymerization.<sup>2,31</sup> In brief, PPY is formed by coupling reactions commencing with the pyrrole cations.<sup>2,31</sup> In this study, the UV light applied at  $365\text{ nm}$  is sufficient to excite  $\text{TiO}_2$  NPs and must produce a pair of the conduction-band electron ( $e^-$ ) and valence-band hole ( $h^+$ ), as indicated in reaction (1). Given that the photogenerated hole is a powerful oxidant,<sup>13</sup> we therefore consider the current pyrrole polymerization as a photocatalyzed polymerization due to the oxidative hole. In the following, the reaction sequences are presented, and this mechanism is solidly supported by the results shown in the UV-vis spectra (see Fig. 1).

Pyrrole is oxidized by the photoexcited  $\text{TiO}_2$  NPs by loss of a  $\pi$  electron, giving rise to a pyrrole radical cation, as indicated in reaction (2).



The coupling reaction of two pyrrole cations produces a pyrrole dimer (reaction 3).<sup>2,31</sup> The subsequent coupling reaction of dimer and pyrrole cations gives a terpyrrole. Quarterpyrrole can be produced from the coupling of two dimers or the coupling reaction of terpyrrole and pyrrole cations.

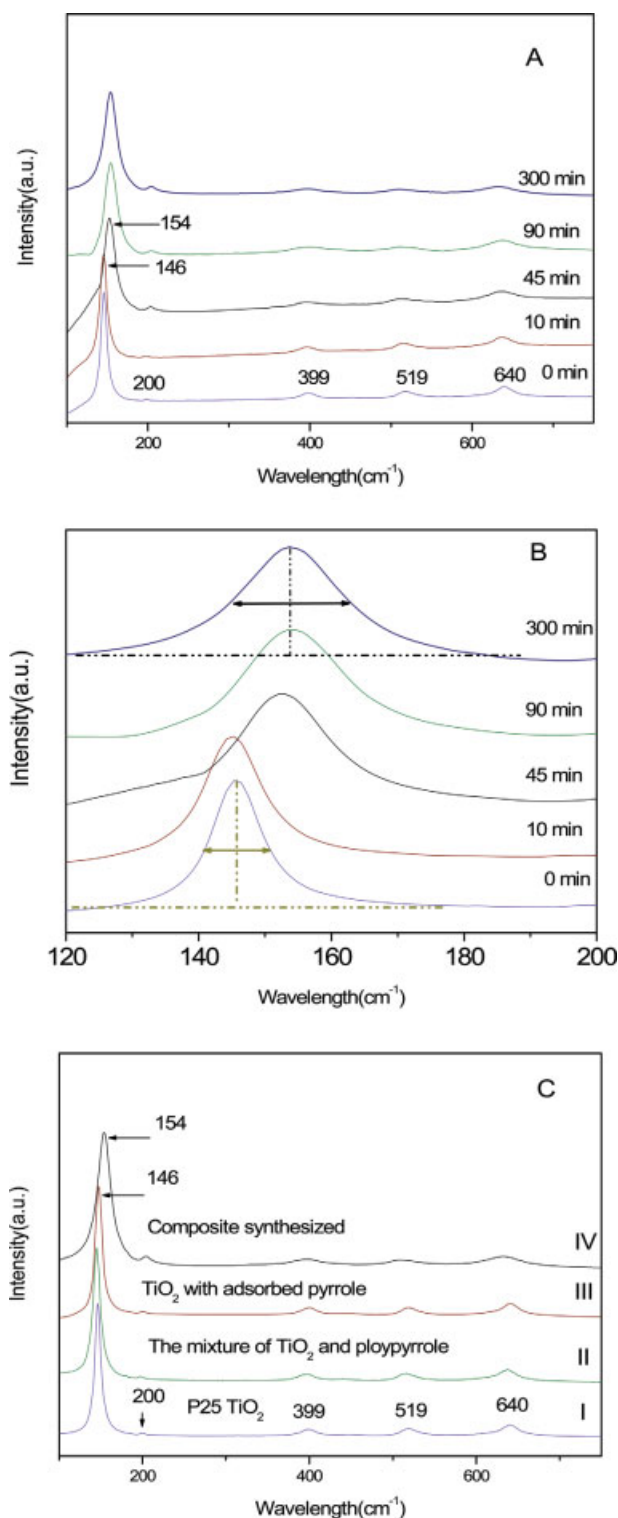


**Figure 5** Raman spectral regions of TiO<sub>2</sub> nanoparticles. (A) the particles obtained after the reactions of different time; (B) high resolution of spectrum (A) in the range of 120–200 cm<sup>-1</sup>; (C) the samples prepared by mixing pure polypyrrole with TiO<sub>2</sub> (Line II) and pyrrole adsorption on TiO<sub>2</sub> (Line III), compared to the neat TiO<sub>2</sub> (Line I) and composite synthesized in this study (Line IV). [Color figure can be viewed in the online issue, which is available at [www.interscience.wiley.com](http://www.interscience.wiley.com).]

**TABLE I**  
The Raman Wavenumbers and FWHM (in bracket) for TiO<sub>2</sub> and the Composite (cm<sup>-1</sup>)

Vibration bands	Neat TiO <sub>2</sub>	Composite
<i>v</i> <sub>6</sub> ( <i>E</i> <sub>g</sub> )	146 (10)	154 (20)
<i>B</i> <sub>1g</sub>	399 (22)	400 (41)
<i>A</i> <sub>1g</sub>	519 (25)	519 (43)
<i>E</i> <sub>g</sub>	639 (26)	639 (51)

Note that the dimer, terpyrrole, and quarterpyrrole are clearly observed in the UV-vis spectra of the reacted mixture (Fig. 1). Above coupling reactions, they are proceeded step-by-step with the formation of PPy eventually,<sup>2,31</sup> as shown in reaction (4).

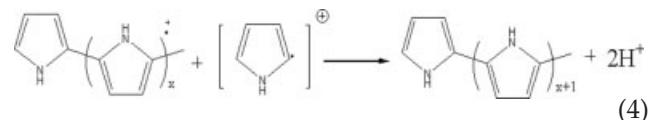
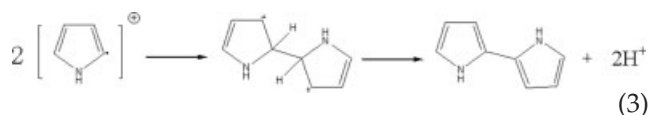


Figure 1(B) shows that the intensity of terpyrrole is considerably weaker than that of quarterpyrrole. We therefore deduce that the dimerization (reaction 3) is very rapid leading to a quick consummation of the pyrrole cations. In this case, the coupling reaction toward terpyrrole is suppressed by the lack of pyrrole cations.

To validate the role of the hole, we carry out the experiments in the presence of methanol, which is known as the hole scavenger in the field of semiconductor chemistry.<sup>32</sup> Lots of researchers have shown that the methanol scavenging on hole is a process that the hole transfers from the oxygen lattice of TiO<sub>2</sub> to methanol.<sup>32</sup>

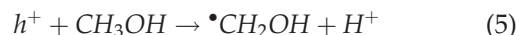
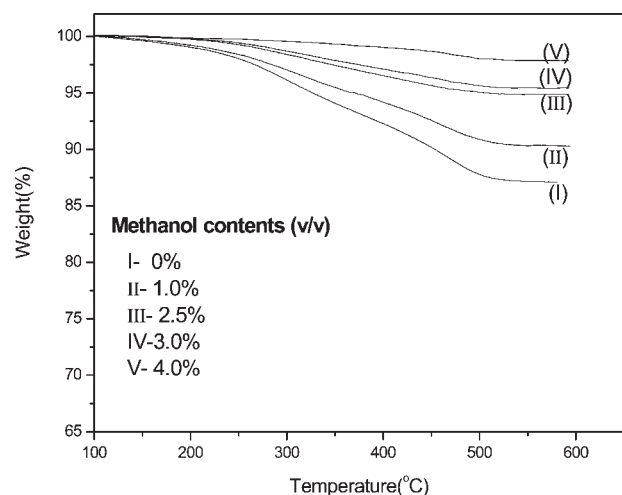


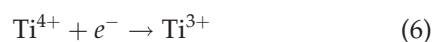
Figure 6 shows that the conversion of pyrrole decreases with increasing the concentration of methanol added. On calculation, the polymer yield sharply decreases from 16% to 1% when methanol of 4% by volume is added. This result can be regarded as that 95% of holes are scavenged at this condition. When the concentration of methanol is further increased, the polymer yield keeps almost unchanged. This agrees with the results by other authors that ~ 5–10% of the holes are remained even at high concentrations of hole scavengers.<sup>33</sup> Conclusively, above results confirm that pyrrole is initiated by the photogenerated hole.



**Figure 6** TGA curves of the composite obtained at various concentrations of methanol as the hole scavenger. The concentration of  $\text{TiO}_2$  was 0.75 g/L. The concentration of pyrrole was 0.01 mol/L.

Back to Figure 5(C), one can see that the pyrrole adsorption and the mixing of pure PPy with  $\text{TiO}_2$  do not bring about visible changes to the Raman vibrations of  $\text{TiO}_2$  NPs, whereas the two samples have the same wavenumbers and FWHM as those of the neat  $\text{TiO}_2$ . Therefore, we conclude that the interaction between the two components has no relation to the adsorption, whereas the interaction is built up during the photocatalytic reaction. Because of strong interaction, this composite is expected to have a stable interface, and thus, it is promising for practical applications, because long-lived photoelectric devices require the composites with a stable interface structure.

Because the interaction is induced by the photocatalytic reaction, the photogenerated charge carriers must be taken into account. As well known, the electron is trapped by the  $\text{TiO}_2$  NPs, converting  $\text{Ti}^{4+}$  to  $\text{Ti}^{3+}$ .<sup>13</sup>



It is realized, in this discussion, that the  $\text{Ti}^{3+}$  occurs along with the formation of reactive oxygen vacancy defect, as indicated by the reactions with  $\text{NH}_3$ , ethylamine, and sulfur.<sup>34–36</sup> It has been shown that the reaction should be defined as an exchange reaction at the position of oxygen vacancy defect, and the resulted bonding is best described as covalent.<sup>35</sup> On the basis of the earlier achievements, it is most likely that the photoinduced interaction here is attributed to the reactivity along with the  $\text{Ti}^{3+}$ . If it is true that the  $\text{TiO}_2$  is covalently bonded by the pyrrole ring, the surface structure of  $\text{TiO}_2$  should turn aside from its original stoichiometry.<sup>37</sup> In this case, the Raman shift and broadening detected for the  $\text{TiO}_2$  is soundly interpreted in terms of nonstoichi-

ometry, whereas the strong interaction is also clarified.

## CONCLUSIONS

The oxidative polymerization of pyrrole is achieved by using UV-excited  $\text{TiO}_2$  nanoparticles as initiators. The pyrrole oligomers (dimmer, terpyrrole, and quarterpyrrole) and PPy are continuously produced with reaction time. The conversion of pyrrole changes as a function of the concentration of  $\text{TiO}_2$ . It is found that PPy in the composites has the conjugated structure, and the polymer is partially oxidized with the formation of positively charged  $\text{N}^+$ . From the ratio, the peak area of  $\text{N}^+$  to that of total N 1s orbital, it is calculated that the ratio of  $\text{N}^+$  is about 20% after the polymerization of 45 min. The results from XPS and Raman analysis consistently indicate that strong interaction is established between  $\text{TiO}_2$  and the resulting polymer. The comparisons distinguish this interaction from adsorption and conclude that it is built up due to the photocatalytic reaction. It is further discussed that the interaction is related to the reactivity of the  $\text{Ti}^{3+}$  generated from the electron reaction. The mechanism about the polymerization is proposed based on the results of UV-vis spectroscopy. It is drawn that the dimmerization is very rapid. The scavenging experiments with methanol identify that pyrrole is initiated by the hole.

The help from Associated Prof. Xinghai Yu, Faculty of Inorganic Materials Chemistry, Fudan University, in analysis of  $\text{TiO}_2$  is appreciated.

## References

- Zhang, F. L.; Johansson, M.; Andersson, M. R.; Hummelin, J. C.; Inganäs, O. *Adv Mater* 2002, 14, 662.
- Feast, W. J.; Tsibouklis, J.; Pouwer, K. L.; Groenendaal, L.; Meijer, E. W. *Polymer* 1996, 37, 5017.
- Pomogailo, A. D. *Inorg Mater* 2005, 41, S47.
- Godvosky, D. Y. *Adv Polym Sci* 2000, 153, 163.
- Dimitrakopoulos, C. D.; Malenfant, P. R. L. *Adv Mater* 2002, 14, 999.
- Jesus, M. C.; Fu, Y.; Weiss, R. A. *Polym Eng Sci* 1997, 37, 1936.
- Guyard, L.; Hapiot, P.; Neta, P. *J Phys Chem* 1997, 101, 5698.
- Senadeera, G. K. R.; Kitamura, T.; Wadab, Y.; Yanagida, S. *J Photochem Photobiol A Chem* 2006, 184, 234.
- Flitton, R.; Johal, J.; Maeda, S.; Armes, S. P. *J Colloid Interf Sci* 1995, 173, 135.
- Chowdhury, D.; Paul, A.; Chattopadhyay, A. *Langmuir* 2005, 21, 4123.
- Vermeir, I. E.; Kim, N. Y.; Laibinis, P. E. *Appl Phys Lett* 1999, 74, 3860.
- Shoute, L. C. T.; Loppnow, G. R. *J Am Chem Soc* 2003, 125, 15636.
- Hoffman, M. R.; Martin, S. T.; Choi, W.; Bahnemann, D. W. *Chem Rev* 1995, 95, 69.
- Dong, C.; Ni, X. Y. *J Macromol Sci A* 2004, 41, 547.
- Ye, J.; Ni, X. Y.; Dong, C. *J Macromol Sci A* 2005, 42, 1451.

16. Ni, X. Y.; Ye, J.; Dong, C. *J Photochem Photobiol A Chem* 2006, 181, 19.
17. Hoffman, A. J.; Mills, G.; Yee, H.; Hoffman, M. R. *J Phys Chem* 1992, 96, 5540.
18. Stroyuk, A. L.; Granchak, V. M.; Korzhak, A. V.; Kuchmii, S. Y. *J Photochem Photobiol A Chem* 2004, 162, 339.
19. Zotti, G.; Martina, S.; Weger, G.; Schluter, A. D. *Adv Mater* 1992, 4, 798.
20. Langsdorf, B. L.; Maclean, B. J.; Halfyard, J. E.; Hughes, J. A.; Pickup, P. G. *J Phys Chem B* 2003, 107, 2480.
21. Reece, D. A.; Pringle, J. M.; Ralph, S. F.; Wallace, G. G. *Macromolecules* 2005, 38, 1616.
22. Neoh, K. G.; Lau, K. K.; Wong, V. V. T.; Kang, E. T.; Tan, K. L. *Chem Mater* 1996, 8, 167.
23. Kim, D. Y.; Lee, J. Y.; Kim, C. Y.; Kang, E. T.; Tan, K. L. *Synth Met* 1995, 72, 243.
24. Batz, P.; Schmeisser, D.; Gopel, W. *Phys Rev B* 1991, 43, 9178.
25. Zhang, W. X.; Wen, X. G.; Yang, S. H. *Langmuir* 2003, 19, 4420.
26. Ohsaka, T.; Izumi, F.; Fujiki, Y. *J Raman Spectrosc* 1978, 7, 321.
27. Parker, J. C.; Siegel, R. W. *Appl Phys Lett* 1990, 57, 943.
28. Bacsá, R.; Kiwi, J.; Ohno, T.; Albers, P.; Nadtochenko, V. *J Phys Chem B* 2005, 109, 5994.
29. Li, Y. L.; Ishigaki, T. *J Phys Chem B* 2004, 108, 15536.
30. Wang, X. H.; Li, J. G.; Kamiyama, H.; Katada, M.; Ohashi, N.; Moriyoshi, Y.; Ishigaki, T. *J Am Chem Soc* 2005, 127, 10982.
31. De Jesus, M. C.; Fu, Y.; Weiss, R. A. *Polym Eng Sci* 1997, 37, 1936.
32. Du, Y. D.; Rabani, J. *J Phys Chem B* 2003, 107, 11970.
33. Shkrob, I. A.; Sauer, M. C., Jr. *J Phys Chem B* 2004, 108, 12497.
34. Farfan-Arribas, E.; Madix, R. J. *J Phys Chem B* 2003, 107, 3225.
35. Rodriguez, J. A.; Hrbek, J.; Chand, Z. P.; Dvoak, J.; Jiirsak, T. *Phys Rev B* 2002, 65, 235414.
36. Giordano, L.; Goniakowski, J.; Pacchioni, G. *Phys Rev B* 2001, 64, 075417.
37. Di Valentin, C.; Pacchioni, G.; Selloni, A.; Livraghi, S.; Giamello, E. *J Phys Chem B* 2005, 109, 11415.